October, 1988

Slip, twinning, and fracture at a grain boundary in the L12 ordered structure—AΣ = 9 tilt boundary

Alexander H. King, *Oak Ridge National Laboratory*
M. H. Yoo, *Oak Ridge National Laboratory*

Slip, twinning, and fracture at a grain boundary in the $L1_2$ ordered structure—A $\Sigma = 9$ tilt boundary

M. H. Yoo and A. H. King[a)]
Metals and Ceramics Division, Oak Ridge National Laboratory, Oak Ridge, Tennessee 37831

(Received 25 April 1988; accepted 9 June 1988)

The role of interaction between slip dislocations and a $\Sigma = 9$ tilt boundary in localized microplastic deformation, cleavage, or intergranular fracture in the $L1_2$ ordered structure has been analyzed by using the anisotropic elasticity theory of dislocations and fracture. Screw superpartials cross slip easily at the boundary onto the $(1\bar{1}1)$ and the (001) planes at low and high temperatures, respectively. Transmission of primary slip dislocations onto the conjugate slip system occurs with a certain degree of difficulty, which is eased by localized disordering. When the transmission is impeded, cleavage fracture on the $(\bar{1}11)$ plane is predicted to occur, not intergranular fracture, unless a symmetric double pileup occurs simultaneously. Absorption (or emission) of superpartials occurs only when the boundary region is disordered. Slip initiation from pre-existing sources near the boundary can occur under the local stress concentration. Implications of the present result on the inherent brittleness of grain boundaries in Ni_3Al and its improvement by boron segregation are discussed.

I. INTRODUCTION

Ordered intermetallic compounds of the $L1_2$ structure are generally known to possess high strength at elevated temperatures due to the low atomic mobility and low ductility due to the brittleness of grain boundaries (GBs).[1,2] Much attention has been given to Ni_3Al, in particular, because of two outstanding deformation and fracture characteristics, namely the anomalous (positive) temperature dependence of yield and flow stresses, and the dramatic effect that small additions of boron and deviations from stoichiometry have on intergranular fracture. While there has been notable advancement in the mechanistic understanding of the anomalous yield behavior, the principal cause for the inherent susceptibility to intergranular fracture is elusive and poorly understood.

According to atomistic simulation studies, both at the ground state[3] and at elevated temperatures by an equilibrium Monte Carlo simulation,[4] the cohesive energies of GBs ($\Sigma = 13$ twist and tilt, and $\Sigma = 15$ tilt) are comparable for ductile nickel and brittle Ni_3Al. These results suggest that the intrinsic brittleness of polycrystalline Ni_3Al must be related not only to cohesive strength, but also to other factors such as the efficiency of inhomogeneous plastic deformation at or near GBs.

The glide resistance to mobile dislocations of the active slip system depends critically on the dissociation configurations[5] and the core structure[6–8] of the superdislocations. Analogously, nucleation of a crack at a GB depends crucially on the crystallographic characteristics and the atomic structure of the GB. In single-phase $L1_2$ alloys, the stress concentration necessary for intergranular crack nucleation is likely to occur as a result of the interaction of slip with a GB.

There have been several investigations on slip-GB interactions in $L1_2$ alloys, such as Ni_3Fe (Ref. 9) and Ni_3Al (Refs. 10–12), by direct dynamic observation using *in situ* straining transmission electron microscopy (TEM). In the case of Ni_3Al, however, no consensus has emerged as to the role of the inhomogeneous plastic deformation at GBs in the intrinsic brittleness of polycrystals and the boron ductilizing effect. According to our crystallographic analysis of dislocation reactions at GBs,[13] transmission,[10,11] absorption,[12] and initiation[11,12] of slip dislocations at GBs are all possible depending on the local conditions of GB character and stress state.

We showed earlier[13] that many of the possible dislocation reactions at GBs, absorption (emission) and/or transmission, become energetically unfavorable if chemical coordination must be maintained in the structure of the GB. This can explain, in part, the intrinsic brittleness of polycrystalline Ni_3Al. It was further suggested that the beneficial effect of boron segregation to a GB is to disorder the GB, thus making slip transmission and initiation easier.

The purpose of this article is to choose one specific GB type in the $L1_2$ structure and to carry out the stress analysis necessary for a prediction of slip initiation and/or crack nucleation. A condensed version of this article is to be published in a conference proceedings.[14] The choice of $\Sigma = 9$ symmetric tilt boundary is rationalized in Sec. II. The stress concentration ahead of a slip

a) Permanent address: Department of Materials Science and Engineering, State University of New York at Stony Brook, Stony Brook, New York 11794-2275.

 0003-6951/88/050848-08$01.75

band is given in Sec. III. The energetics and kinetics of slip and crack nucleation are discussed in Sec. IV. Finally, in Sec. V, discussion is given of the limiting assumptions of the present analyses including the dynamic effect of slip–GB interaction.

II. $\Sigma = 9$ TILT BOUNDARY

A $\Sigma = 9$ symmetric tilt boundary with a rotation angle, $\Psi = 38.94°$, about the [110] axis has been chosen for a number of reasons on the basis of crystal symmetry. First, the rotation axis of [110] is appropriate for the $L1_2$ structure because the cross slip of superdislocations of Burgers vector $\mathbf{b} = <110>$ plays an important role in macroscopic yielding and strain hardening. Second, as shown in Fig. 1, the angle between the primary slip plane, $(1\bar{1}1)$, and the boundary plane, $(2\bar{2}\bar{1})$, is the same as that between the octahedral plane, $(1\bar{1}1)$ or $(1\bar{1}\bar{1})$, and the (001) cube cross-slip plane, $\theta = (\Psi + \pi)/4 = \cos^{-1}\sqrt{1/3} = 54.74°$, and the angle between two $\{111\}$ planes is related to θ_1, $\theta_2 = \pi - 2\theta_1 = \cos^{-1}(1/3) = 70.53°$.

The tensile loading axis of a bicrystal is chosen to be $\mathbf{P}_1 = [7,20,\overline{26}]_2 = [20,7,\overline{26}]_2$ as shown in Fig. 1. Three slip systems in crystal (1) with high Schmid factors, m's, are listed in Table I. The primary slip system is $(1\bar{1}1)[\bar{1}01]$ with $m_p = 0.47$. The coordinate system shown in Table I is with respect to the pure screw orientation of a superdislocation.

The third reason for choosing a $\Sigma = 9$ tilt boundary is related to the long-range elastic interaction between a superdislocation and a grain boundary. The interaction exists only in an elastically anisotropic material such as Ni_3Al, Ni_3Fe, or Cu_3Au with a shear anisotropy factor $A = 3.3$, 2.5, or 2.6. When a straight superdislocation lies parallel to an even-fold symmetry axis, e.g., $\mathbf{z} \| [110]$, the edge and screw components of elastic fields are independent of each other.[15] For instance, a mixed (60°) dislocation of the primary slip system may be decomposed into two components, $\mathbf{b} = \mathbf{b}_e + \mathbf{b}_s$, as

$$[\bar{1}01] = \tfrac{1}{2}[\bar{1}12] + \tfrac{1}{2}[\bar{1}\bar{1}0] \,. \tag{1}$$

Whereas, the prelogarithmic energy factor of the screw component is $K_s = [C_{44}(C_{11} - C_{12})/2]^{1/2}$, where C_{11}, C_{12}, and C_{44} are the elastic constants, that of the edge component, K_e, can be obtained numerically.[15] In order to estimate the long-range interaction force F_x, we use the approximate solution that was derived earlier,[16]

$$F_x/B = k(b_e/x) \,, \tag{2}$$

where $B = (K'_e + K_e)b_e/8\pi$, $k = (K'_e - K_e)/(K'_e + K_e)$, K'_e is the energy factor corresponding to $(1\bar{1}1)_1[\bar{1}01]_1$ in crystal (2), and x is the distance from the GB. The interaction is attractive when $k < 0$ and repulsive when $k > 0$.

Numerical results of k as a function of θ are shown in Fig. 2. It is important to note that $k = 0$ at $\theta = 54.74°$ for $\Sigma = 9$. This means that no long-range interaction exists between any straight dislocation that lies parallel to the [110] axis and the $\Sigma = 9$ tilt boundary.

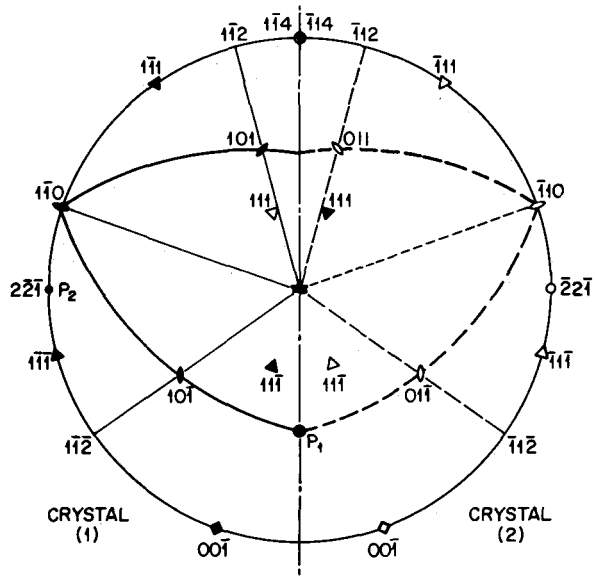

FIG. 1. Stereographic (110) projection of a bicrystal $\Sigma = 9$ symmetric tilt boundary, $\Psi = 38.94°$. The solid lines and filled symbols represent crystal (1). The broken lines and open symbols represent crystal (2). The tensile axis: $\mathbf{P}_1 = [7,20,\overline{26}]_1 = [20,7,\overline{26}]_2$ or $\mathbf{P}_2 = [2\bar{2}\bar{1}]_1 = [\bar{2}2\bar{1}]_2$.

TABLE I. Schmid factors for active slip systems in crystal (1).

Slip plane x_2	Slip direction x_3	m_p	h x_1	m_e	Cross slip x'_2	m_e
(a) $(1\bar{1}1)$	$[\bar{1}01]$	0.47	$[\bar{1}\bar{2}\bar{1}]$	0.17	(010)	−0.41
(b) $(1\bar{1}1)$	$[\bar{1}\bar{1}0]$	0.38	$[1\bar{1}\bar{2}]$	−0.32	(001)	0.44
(c) $(11\bar{1})$	$[\bar{1}0\bar{1}]$	0.37	$[\bar{1}21]$	−0.08	(010)	−0.24

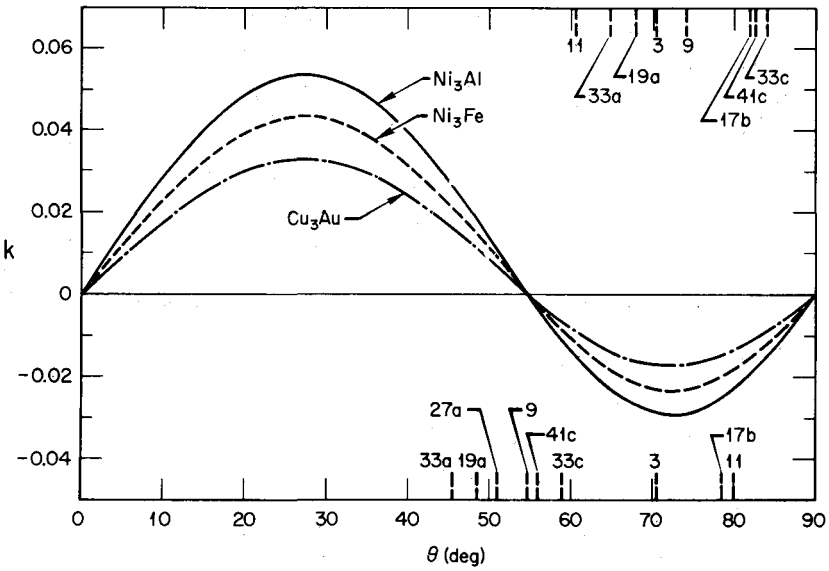

FIG. 2. The elastic interaction between $(1\bar{1}1)[\bar{1}01]$ slip and a symmetric tilt boundary with the [110] rotation axis. Here θ is the angle between the $(1\bar{1}1)$ plane and the boundary plane.

III. STRESS ANALYSIS

The theory of dislocation pileups was reviewed by Chou and Li.[17] In reference to the polar coordinate system (r,ϕ), defined at the head of a single-ended pileup as shown in Figs. 3 and 4, the three stress components are

$$\frac{\sigma_{\phi\phi}}{\tau\alpha_e} = \left(\frac{l}{r}\right)^{1/2} \cdot f_{\mathrm{I}}(\phi), \quad f_{\mathrm{I}} = \tfrac{3}{2}\sin\phi\cos\frac{\phi}{2}, \tag{3}$$

$$\frac{\sigma_{r\phi}}{\tau\alpha_e} = \left(\frac{l}{r}\right)^{1/2} \cdot f_{\mathrm{II}}(\phi),$$

$$f_{\mathrm{II}} = \tfrac{1}{2}\left(2\cos\frac{3\phi}{2} + \sin\phi\sin\frac{\phi}{2}\right), \tag{4}$$

$$\frac{\sigma_{\phi z}}{\tau\alpha_s} = -\left(\frac{l}{r}\right)^{1/2} \cdot f_{\mathrm{III}}(\phi), \quad f_{\mathrm{III}} = 2\cos\frac{\phi}{2}, \tag{5}$$

where τ is an effective shear stress defined as the difference between the applied shear stress τ_{ij} and the glide resistance τ_0, and the pileup length is $l = D/2\tau$. The general expressions of τ and D for a mixed dislocation of Burgers vector **b** are

$$\tau = \tau_{xy}\sin\beta + \tau_{yz}\cos\beta - \tau_0, \tag{6}$$

$$D = (b/2\pi)(K_e\sin^2\beta + K_s\cos^2\beta), \tag{7}$$

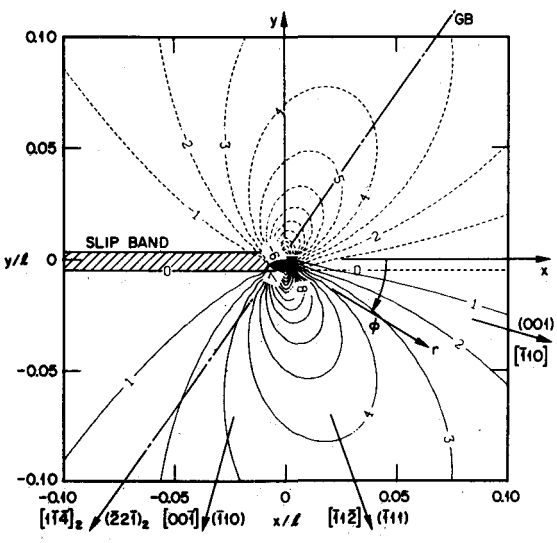

FIG. 3. Equistress contour plot of $\sigma_{\phi\phi}/\tau\alpha_e$.

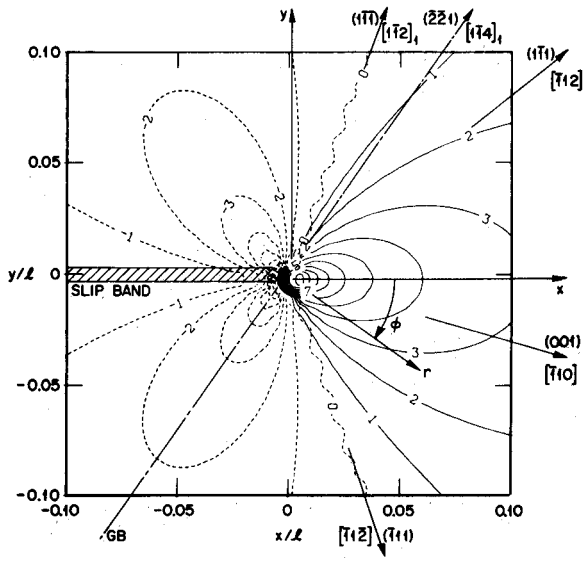

FIG. 4. Equistress contour plot of $\sigma_{r\phi}/\tau\alpha_e$.

where β is the angle between **b** and the dislocation line **z**. Numerical factors of $\alpha_e = D_e/D$ and $\alpha_s = D_s/D$ are also needed.

Equistress contour plots of $\sigma_{\phi\phi}/\tau\alpha_e$ and $\sigma_{r\phi}/\tau\alpha_e$ are shown in Figs. 3 and 4. The cross-hatched band indicates the front end of a dislocation pileup, and this lies in crystal (1) which is to the left of the $\Sigma = 9$ tilt boundary marked by a center line.

For the edge component, the shear stress is largest directly ahead of the pileup as shown in Fig. 4, $f_{\mathrm{II}} = 1$ when $\phi = 0$, and it vanishes at $\phi = \cos^{-1}(1/3) = 70.53°$. Conversely, the normal stress is largest in tension, $f_{\mathrm{I}} = 2/\sqrt{3}$, at $\phi = 70.53°$, and it is zero at $\phi = 0°$. The state of maximum $\sigma_{\phi\phi}$ and zero $\sigma_{r\phi}$ occurs on $(\bar{1}11)_2$, the primary slip plane of crystal (2). As for the screw component, the pure shear stress, $\sigma_{\phi z}$, is maximum with $f_{\mathrm{III}} = 2$ when $\phi = 0$.

IV. SLIP, TWIN, AND CRACK INITIATION

A multitude of deformation and fracture modes can be considered with the aid of Figs. 3 and 4 and Table II. In each category, the initiation probability is discussed in terms of the energetics and kinetics involved in the process. For all the slip systems in crystal (1), it is assumed that each superdislocation is dissociated into two identical superpartials bounding an antiphase boundary (APB). In this section, we assume further that chemical state of the $L1_2$ structure at the GB region is fully ordered.

A. Cross slip

According to the definition given earlier,[13] a screw superpartial of the Burgers vector, $1/2[\bar{1}\bar{1}0]$, cannot be absorbed into the GB, but its transmission across the boundary is possible without leaving any residual Burgers vectors in the boundary. The cross-slip reaction is

$$\tfrac{1}{2}[\bar{1}\bar{1}0]_1 \rightarrow \tfrac{1}{2}[\bar{1}\bar{1}0]_2 . \qquad (8)$$

There are three potential cross-slip planes, $(1\bar{1}1)$, (001), and $(\bar{1}11)$. The values of $m_e = 0.44$ and $f_{\mathrm{III}} = 1.96$ are both highest in the (001) plane, as listed in Tables I and II, respectively. In view of the low mobility of screw superdislocations on the (001) plane,[6,7] however, this $(1\bar{1}1)_1$–$(001)_2$ cross slip is expected to occur only at elevated temperatures.

B. Secondary slip

Again, absorption of $1/2[\bar{1}01]$ is not possible. For a mixed superpartial of $b = 1/2[011]_2$ or $b = 1/2[01\bar{1}]_2$ with $\beta = 60°$, we find from Eq. (7) that the orientation factor is $f_s = [(\alpha_e f_{\mathrm{II}})^2 + (\alpha_s f_{\mathrm{III}})^2]^{1/2}$ with $\alpha_e = 3K_e/(3K_e + K_s)$ and $\alpha_s = K_s/(3K_e + K_s)$.

Using $K_e = 115$ GPa and $K_s = 68$ GPa for Ni_3Al (Ref. 18), we find $\alpha_e = 0.83$ and $\alpha_s = 0.17$, which yield $f_s = 0.61$ and $f_s = 0.28$ for the two cases (2) and (4), respectively, in Table II.

Consequently, the most probable transmission reaction is

$$\tfrac{1}{2}[\bar{1}01]_1(1\bar{1}1)_1 \rightarrow \tfrac{1}{2}[011]_2(1\bar{1}1)_2 + \mathbf{b}_{\mathrm{B}} , \qquad (9)$$

where $\mathbf{b}_{\mathrm{B}}$ is the sum of Burgers vectors of the perfect extrinsic grain boundary dislocations (EGBDs) which are necessarily the translation vectors of the DSC lattice. (The DSC lattice is so called because of displacements of one crystal with respect to the other that shift the boundary structure, but leave it complete, or unchanged.) The residues at the boundary are

$$\mathbf{b}_{\mathrm{B}} = \tfrac{1}{9}[\bar{2}21]_{\mathrm{B}} - \tfrac{1}{9}[542]_{\mathrm{B}} , \qquad (10)$$

where both vectors contain climb components perpendicular to the $\Sigma = 9$ tilt boundary, $(2\bar{2}\bar{1})_1 = (\bar{2}2\bar{1})_2$. This means that the kinetics of a sequential transmission of superpartials depends on the climb mobility of those EGBDs that result from the first interaction, and hence on temperature.

TABLE II. Orientation dependence of the stress concentration in crystal (2) due to a dislocation pileup of primary slip in crystal (1).

	ϕ (degree)	f_{I}	f_{II}	f_{III}	Orientation ($\sigma_{r\phi}$)
(1)	−54.7	−1.09	0.32	1.78	$(2\bar{2}1)[1\bar{1}4]_1$
(2)	−39.0	−0.89	0.63	1.88	$(1\bar{1}1)[1\bar{1}2]$
(3)	15.8	0.40	0.93	1.98	$(001)[\bar{1}10]$
(4)	70.5	1.15	0	1.63	$(\bar{1}11)[\bar{1}1\bar{2}]$
(5)	105.8	0.87	−0.55	1.21	$(\bar{1}10)[00\bar{1}]$
(6)	125.3	0.56	−0.63	0.92	$(\bar{2}2\bar{1})[\bar{1}\bar{1}4]_2$

C. Twin

Twin formation at the head of a pileup is a possibility. One possible transformation reaction is

$$\tfrac{1}{2}[\bar{1}01]_1(1\bar{1}1)_1 \rightarrow -\tfrac{1}{6}[211]_2(\bar{1}11)_2 + \mathbf{b}_B\,, \quad (11)$$

$$\mathbf{b}_B = \tfrac{1}{9}[\bar{2}21]_B + \tfrac{1}{9}[1\bar{1}4]_B\,. \quad (12)$$

[When the magnitude of the resultant vector in crystal (2) is different from that of the original vector in crystal (1), the reaction is called transformation.[19]] Nucleation of a three-layer microtwin requires a rather intricate and conducive movement of dislocations involved in four such reactions. In this case, the orientation factor is, $f_T = 0.28$, lower than $f_s = 0.61$ for the secondary slip. Twin formation is, therefore, energetically unfavorable as compared to the initiation of secondary slip. If it ever occurs, the order (complementary) twinning is kinetically more likely than the fcc (primary) twinning.[20]

D. Cleavage

Smith and Barnby[21] developed a nucleation criterion for mode-I crack including the effect of local shear stress, $\sigma_{r\phi}$. The most general criterion for nucleation of a mixed mode crack in crystal (2) caused by a dislocation pileup in crystal (1) under the effective stress τ is

$$\tau_{CR} = \pi(D/l)^{1/2}[\gamma(\phi)/G(\phi)]^{1/2}\,, \quad (13)$$

$$G(\phi) = (\alpha_e f_I)^2 + (\alpha_e f_{II})^2 + (\alpha_s f_{III})^2\,, \quad (14)$$

where $\gamma(\phi)$ is the effective fracture surface energy.

We consider the three possible cleavage planes, (001), $(\bar{1}11)$, and $(\bar{1}10)$, with $f_I > 0$ as shown in Table II. The free-surface energies of these planes have been calculated for Ni_3Al (Ref. 22). These values and the calculated orientation factors are listed in Table III. The lower the value of γ/G, the easier the cleavage nucleation would be. Cleavage is most likely on the $(\bar{1}11)_2$ plane. As long as the effective fracture surface energy has the free-surface energy value throughout the crack initiation process, once a crack is nucleated, it will extend automatically.[21]

E. Intergranular fracture

For the nucleation of a crack on a GB, we use Eq. (13) by replacing γ with $\gamma_c/2$, the cohesive energy of the boundary. Calculating to obtain $G = 0.52$ from Eq. (14) and case (6) of Table II, and assuming $\gamma_c = 3.0$ J/m^2 for the $\Sigma = 9$ tilt boundary,[3] we find $\gamma/G = 2.88$. This is higher than any value for cleavage fractures listed in Table III. Therefore, as compared to the $(\bar{1}11)_2$ cleavage, the initiation of a crack on the $\Sigma = 9$ tilt boundary is not feasible.

TABLE III. The surface energies[21] and the orientation factors for cleavage fracture in Ni_3Al.

Cleavage plane	γ (J/m^2)	G	γ/G
(001)	1.62[a]	0.83	1.95
	1.89[b]		2.23
$(\bar{1}11)$	1.65	1.00	1.65
$(\bar{1}10)$	1.73[a]	0.77	2.25
	1.92[b]		2.49

[a] The mixed composition plane.
[b] The pure Ni plane.

The critical stress for intergranular cavity nucleation was derived earlier,[23]

$$\tau_{CV} \simeq \left(\frac{1}{l}\right)^{1/2}\left(\frac{K_e}{k_B T}\right)^{1/6}\left(\frac{\gamma F_v^{1/3}}{f_I}\right), \quad (15)$$

where k_B is the Boltzman factor, T is the absolute temperature, and F_v is the geometrical factor for a spherically capped cavity embryo.[24] Using a nominal value of $\gamma F_v^{1/3} = 0.5$–1.3 J/m^2, it can be predicted from Eqs. (13)–(15) that cavity nucleation becomes more favorable than crack initiation, i.e., $\tau_{CV} < \tau_{CR}$, at elevated temperatures, $T > 0.4\ T_m$, where T_m is the absolute melting point.

F. Primary slip

Primary slip in crystal (2) can be initiated from a pre-existing dislocation source of Frank–Read type near the GB. If it is assumed that the two $1/2[01\bar{1}]_2$ superpartials of the $(\bar{1}11)_2$ primary slip with $m_p = 0.47$ are nucleated sequentially, the most difficult step must be the bowing out of the first against the APB. The critical shear stress to operate such a Frank–Read source is[25]

$$\tau_{FR} = \lambda(\eta D/l_0 + \gamma_1/b)\,, \quad (16)$$

where l_0 is the distance between pinning points, γ_1 is the APB energy, $\eta = \ln(l_0/b)$, and λ is a stress concentration factor. In the present case, around the head of a dislocation pileup, one finds from Eqs. (4) and (5) that $\lambda = (r/l)^{1/2}/f_s$. It is important to note that the critical stress depends not only on the length of l_0, but also on the stability of the pinning points.

V. DISCUSSION

It is appropriate to discuss the localized slip and fracture initiation, predicted by the present analysis, pertaining to Ni_3Al in the temperature range $T = 77$–300 K because of the following reasons: (1) the dramatic ductilizing effects of boron and deviations from stoi-

chiometry are pronounced at room temperature,[26,27] (2) the input parameters used in Sec. IV are valid for $T < 300$ K, viz. the surface and cohesive energies,[3,4] and (3) the anomalous thermal strengthening is not too high at $T < 300$ K to obscure the present analysis since the peak temperature is $T_p \doteq 900$ K.[25]

When a bicrystal is stressed in tension along $\mathbf{P}_1 = [7,20,\overline{26}]_1 = [20,7,\overline{26}]_2$, as a result of the interaction between the primary slip band and the GB, the following three distinct types of reaction may occur: (a) transmission of $1/2[\bar{1}01]_1(1\bar{1}1)_1$ into $1/2[011]_2(1\bar{1}1)_2$, (b) $(\bar{1}11)_2$ cleavage, or (c) cross slip of $1/2[\bar{1}\bar{1}0]$ from $(1\bar{1}1)_1$ to $(\bar{1}11)_2$. These are schematically shown in Fig. 5(a).

Alternatively, when the tensile axis is directed perpendicular to the GB, i.e., $\mathbf{P}_2 = [2\bar{2}\bar{1}]_1 = [\bar{2}2\bar{1}]_2$, the Schmid factor for any plane containing $1/2[110]$ vanishes, hence no cross slip (c). While transmission (a) or cleavage (b) can occur, as shown in Fig. 5(b), the driving force for these processes is weakened somewhat by the lower Schmid factor for the primary slip ($m_p = 0.41$), in this case (P_2) as compared to that ($m_p = 0.47$) in the previous case ($\mathbf{P}_1$), or equivalently by the reduced effective shear stress, τ, because $\tau_{yz} = 0$ in Eq. (6).

The most important result of the present analysis is the prediction of $(\bar{1}11)_2$ cleavage fracture in the case of the mixed mode I and III. As was discussed in Sec. IV, the orientation-dependent parameters are $\gamma/G = 2.88$ and 1.65 for intergranular and cleavage fracture, respectively, such that the ratio of critical stresses for these two modes is obtained from Eq. (13) to be only 1.32. In a symmetric bicrystal, simultaneous impingement of the primary slip bands from both sides of the GB may occur with some frequency. When such a symmetric double pileup occurs, nucleation of a GB crack can be effected as shown by (d) in Fig. 5.

Formally, absorption and emission belong to the same type of dislocation reactions at GBs. The only difference is that the latter requires the presence of a sufficient number of appropriate GBDs as a precursor. Since neither a $1/2[110]$ dislocation, nor a $1/2[\bar{1}01]$ dislocation can be absorbed into a $\Sigma = 9$ tilt boundary, this boundary when fully ordered does not act as a source of slip dislocations. When the GB region is disordered, however, either dislocation can be absorbed into the boundary, and conversely dislocation emission from it is possible.

The transmission reaction of Eq. (9) becomes energetically more favorable when the GB region is disordered because of the further dissociation of one of the GBDs in Eq. (10) as

$$\tfrac{1}{9}[542]_B \rightarrow \tfrac{1}{18}[363]_B + \tfrac{1}{18}[721]_B \,. \qquad (17)$$

According to the b^2 sum criterion, the energy reduction is 34%. Therefore, from the crystallographic and energetic point of view, both absorption (or initiation) and transmission reactions are greatly enhanced by disordering of the GB region.

It is now well established from Auger electron spectroscopy,[27-29] atom probe,[30-33] and atomistic simulation[34] studies that boron segregates to grain boundaries. There have been a number of experimental correlations for synergistic cosegregation of boron and nickel to GBs and associated local disordering. A circumstantial evidence by atom probe-field ion microscopy (AP-FIM) was found that boron was associated with a thin second phase (less well ordered) at GBs.[30,31] Another AP-FIM experiment on boron-doped Ni_3Al showed a high boron

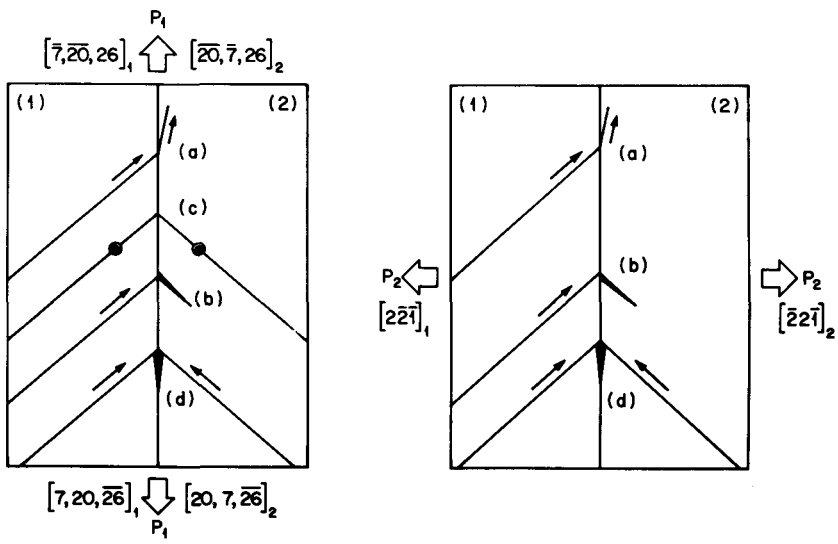

FIG. 5. Schematic illustration of slip and crack initiation at a $\Sigma = 9$ symmetric tilt boundary: (a) transmission, (b) cleavage, (c) cross slip, and (d) intergranular fracture.

concentration along with a depletion of aluminum at a GB.[32] An increase in nickel concentration at a GB with increasing boron concentration was observed by scanning transmission electron microscopy (STEM) analysis.[35] The electron backscatter diffraction analysis of the Burgers vector of the dislocation network in a low-angle twist boundary of boron-doped substoichiometric Ni_3Al was determined to be 1/2[110], which suggests either the presence of APBs or disordering in the vicinity of the boundary.[36] These experimental findings of localized disordering are consistent with various theoretical modeling analyses, the hard sphere model,[37] the embedded atom method (EAM),[3,4,34] and the cluster variation method (CVM).[38,39]

It was shown earlier[13] that in the class of $\Sigma = 3N$ (integer N) boundaries, both the number of allowed absorption and the number of transmission reactions were reduced by a factor of four when the DSC lattice appropriate to the fcc structure (disordered) is changed to the primitive cubic DSC set (ordered). It is not clear how typical the present result on $\Sigma = 9$ tilt boundary is in representing the mechanical behavior of the $\Sigma = 3N$ class. The recent studies on GB-type distribution in polycrystalline Ni_3Al (Refs. 36, 40, 41) showed that the most abundant type is $\Sigma = 3$, and it showed strong resistance against integranular fracture. The frequency of $\Sigma = 9$ was too low to discern apparent resistance against intergranular fracture.[40]

A full understanding of the interaction between a superdislocation and a GB depends not only on the relative energies of the reaction products, but also their mobility under the influence of local stress concentration. According to the recent theory,[42] for instance, the mobility of a screw superdislocation depends on the sense and magnitude of the so-called nonglide stress (τ_{xy}). For example, in Table I the sign of m_e (the Schmid factor on the edge component) indicates either an APB-type dissociation when $m_e > 0$, or a superlattice intrinsic stacking fault (SISF)-type dissociation when $m_e < 0$. This means that the primary slip system (a) is relatively more mobile than the others, (b) and (c). With this theoretical model,[42] the treatment of dynamic dislocation pileup and the diffusional relaxation along the grain boundary[23] can be extended for the $L1_2$ structure. Within the GB region, in which the core of a superpartial and the GB structure overlap, a detailed understanding of the short-range interaction and the intermediate defect structures[43] is needed.

VI. SUMMARY AND CONCLUSIONS

(1) The choice of the $\Sigma = 9$ symmetric tilt boundary was made on the basis of crystal symmetry, including the fact that no long-range elastic interaction exists between any straight dislocation and the boundary.

(2) Cross slip of screw superpartials at the boundary is an easy process. The favored cross-slip plane is the $(\bar{1}11)$ plane at low and intermediate temperatures, or the (001) plane at high temperatures.

(3) The transmission of the primary slip dislocations across the boundary into the conjugate slip system occurs with a certain degree of difficulty, which is eased by localized disordering.

(4) The critical stress criterion for nucleation of a general mixed mode crack at the head of a dislocation pileup was obtained by using the anisotropic elasticity theory of dislocation and fracture.

(5) Unless a symmetric double pileup occurs simultaneously, cleavage fracture on the $(\bar{1}11)$ plane is predicted, not intergranular fracture.

(6) Dislocation absorption (or emission) is possible only when the boundary region is disordered. Slip initiation from pre-existing sources near the boundary can occur under the local stress concentration.

ACKNOWLEDGMENT

Research sponsored by the Division of Materials Science, United States Department of Energy, under Contract DE-AC05-840R21400 with Martin Marietta Energy Systems, Inc.

REFERENCES

[1] *Proceedings of the MRS Symposium on High-Temperature Ordered Intermetallic Alloys*, edited by C. C. Koch, C. T. Liu, and N. S. Stoloff (Materials Research Society, Pittsburgh, PA, 1985).
[2] *Proceedings of the MRS Symposium on High-Temperature Ordered Intermetallic Alloys II*, edited by N. S. Stoloff, C. C. Koch, C. T. Liu, and O. Izumi (Materials Research Society, Pittsburgh, PA, 1987).
[3] S. P. Chen, A. F. Voter, and D. J. Srolovitz, Ref. 2, p. 45.
[4] S. M. Foiles, Ref. 2, p. 51.
[5] M. H. Yoo, Acta Metall. **35**, 1559 (1987).
[6] M. Yamaguchi, V. Paidar, D. P. Pope, and V. Vitek, Philos. Mag. A **45**, 867 (1982).
[7] V. Paidar, M. Yamaguchi, D. P. Pope, and V. Vitek, Philos. Mag. A **45**, 883 (1982).
[8] M. H. Yoo, M. S. Daw, and M. I. Baskes, in *Atomistic Modeling of Materials: Beyond Pair Potentials*, ASM-World Materials Congress, 25–30 Sept., Chicago, IL (1988) (to be published).
[9] G. T. Brown, R. E. Smallman, and D. G. Morris, Phys. Status Solidi A **62**, 509 (1980).
[10] E. M. Schulson, T. P. Weihs, I. Baker, H. J. Frost, and J. A. Horton, Acta Metall. **34**, 1395 (1986).
[11] I. Baker, E. M. Schulson, and J. A. Horton, Acta Metall. **35**, 1533 (1987).
[12] G. M. Bond, I. M. Robertson, and H. K. Birnbaum, J. Mater. Res. **2**, 436 (1987).
[13] A. H. King and M. H. Yoo, Ref. 2, p. 99.
[14] M. H. Yoo and A. H. King, in *Proceedings of the MRS Symposium on Interfacial Structure, Properties, and Design*, 5–8 April 1988, edit-

ed by M. H. Yoo, W.A.T. Clark, and C. L. Briant (Materials Research Society, Pittsburgh, PA) (to be published).
[15]M. H. Yoo and B. T. M. Loh, J. Appl. Phys. **41**, 2805 (1970).
[16]M. H. Yoo, Trans. TMS-AIME **245**, 2051 (1969).
[17]Y. T. Chou and J. C. M. Li, in *Mathematical Theory of Dislocations*, edited by T. Mura (ASME, New York, 1969), p. 116.
[18]M. H. Yoo, Scr. Metall. **20**, 915 (1986).
[19]A. H. King, in *Interface Migration and Control of Microstructure*, edited by C. S. Pande, D. A. Smith, A. H. King, and J. Walder, (American Society for Metals, Metals Park, OH, 1986).
[20]S. B. Chakrabortty and E. A. Starke, Jr., Acta Metall. **23**, 63 (1975).
[21]E. Smith and J. T. Barnby, J. Metall. Sci. **1**, 56 (1967).
[22]S. M. Foiles and M. S. Daw, J. Mater. Res. **2**, 5 (1987).
[23]M. H. Yoo and H. Trinkaus, Acta Metall. **34**, 2381 (1986).
[24]R. Raj and M. F. Ashby, Acta Metall. **23**, 653 (1975).
[25]C. Lall, S. Chin, and D. P. Pope, Metall. Trans. A **10**, 1323 (1979).
[26]K. Aoki and 0. Izumi, Nippon Ginzoku Gakkaish **43**, 1190 (1979).
[27]C. T. Liu, C. L. White, and J. A. Horton, Acta Metall. **33**, 213 (1985).
[28]C. L. White, R. A. Padgett, C. T. Liu, and S. M. Yalisgrove, Scr. Metall. **18**, 1417 (1984).
[29]A. Choudhury, C. L. White, and C. R. Brooks, Scr. Metall. **20**, 1061 (1986).
[30]M. K. Miller and J. A. Horton, Scr. Metall. **20**, 789 (1986).
[31]J. A. Horton and M. K. Miller, Acta Metall. **35**, 133 (1987).
[32]D. D. Sieloff, S. S. Brenner, and M. G. Burke, Ref. 2, p. 87.
[33]J. A. Horton and M. K. Miller, Ref. 2, p. 105.
[34]S. P. Chen, A. F. Voter, and D. J. Srolovitz, J. Phys (Paris) (to be published).
[35]I. Baker, E. M. Schulson, and J. R. Michael, Philos. Mag. B **57**, 379 (1988).
[36]R. A. D. Mackenzie, M. D. Vaudin, and S. L. Sass, in Ref. 14.
[37]H. J. Frost, Acta Metall. **35**, 519 (1987).
[38]R. Kikuchi and J. W. Cahn, Phys. Rev. B **36**, 418 (1987).
[39]D. Farkas and H. Jang, Ref. 2, p. 65.
[40]S. Hanada, T. Ogura, S. Watanabe, 0. Izumi, and T. Masumoto, Acta Metall. **34**, 13 (1986).
[41]D. Farkas, M. O. Lewus, and V. Rangarajan, Scr. Metall. (submitted).
[42]M. H. Yoo, J. A. Horton, and C. T. Liu, Acta Metall. (to be published).
[43]A. H. King and F. R. Chen, J. Mater. Sci. **66**, 227 (1984).